

Population dynamic consequences of variability in age of spawning and survival rates of Pacific salmon

Lee Worden^{a,b,*}, Louis W. Botsford^c, Alan Hastings^b, Matthew D. Holland^c

^a*Department of Biology, Theoretical Biology Lab, McMaster University, LS 332 1280 Main Street West, Hamilton, ON L8S 4K1 Canada*

^b*Department of Environmental Science & Policy, University of California, Davis, One Shields Ave, Davis, California 95616 USA*

^c*Department of Wildlife, Fish, & Conservation Biology, University of California, Davis, One Shields Ave, Davis, California 95616 USA*

Abstract

Recent dramatic changes in the abundance of Pacific salmon, possibly due to fishing or climate change, raise the question of how these density-dependent populations of a semelparous species should be expected to respond to a random environment. Linearizing an age-structured model with density-dependent recruitment about a fixed point showed that the dominant modes of variability are a geometrically decaying mode, a cyclic mode with period equal to the dominant age of reproduction, and a cyclic mode with period 2. Random variability in survival appears to preferentially excite the geometrically decaying mode, while variability in the spawning age preferentially excites the cyclic mode. As mean long-term adult survival declines, all modes of variability increase, indicating greater sensitivity of the population to environmental variability. The relative strength of each mode depends on the type of observation, with total abundance tending to be more skewed toward lower frequencies than recruitment.

Keywords: Variability, Structured populations, Salmon, Noise color

*Corresponding author

Email addresses: worden.lee@gmail.com (Lee Worden), lwbotsford@ucdavis.edu (Louis W. Botsford), amhastings@ucdavis.edu (Alan Hastings), mhdolland@ucdavis.edu (Matthew D. Holland)

1. Introduction

With increasing concern for the effects of fishing and climate change on marine ecosystems, there is an interest in the effects of the marine environment on population dynamics of Pacific salmon on annual and decadal time scales. Analyses of the influences of the ocean environment on Pacific salmon, whether statistical examination of covariability between population and environmental variables (*e.g.*, Logerwell et al., 2003) or estimation of survivals to specific sizes and ages through analysis of coded wire tagging data (*e.g.*, Coronado and Hilborn, 1998; Teo et al., 2009), commonly assume the variable ocean environment influences survival during the early ocean phase of this anadromous genus. There have been fewer cases in which environmental variability in the age of maturation has been analyzed (*e.g.*, Pyper et al., 1999).

These empirical findings raise questions regarding the relative roles of random variability in survival at various ages, and in the age distribution of reproduction, on salmon population dynamics. Random survival is typically assumed to influence abundance directly, but the effects of varying age of spawning are not as clear, and there is a need to understand differences in population response to these two sources of random variability.

Here we examine and compare the effects of environmental variability in survival and age of spawning on the magnitude and time scales of population variability. We are engaged in a study of the influence of the oceanographic environment on Pacific salmon, the GLOBEC North East Pacific program, part of the US Climate Change program. Earlier retrospective analyses indicated differences in the responses of the two California Current congeners, chinook salmon, *Oncorhynchus tshawytscha*, and coho salmon, *O. kisutch*, and hence we are interested in the population dynamic differences between them (Botsford and Lawrence, 2002). These species differ in their age distribution of spawning and in other ways (Botsford et al., 2005). We have explored some of the differences in probabilities of extinction of populations with these spawning age distributions in response to time-varying marine survival (Hill et al.,

2003; Botsford et al., 2005). In salmon, differences in maturity schedule are due to differences in size distribution (and therefore prior growth rate) (Young, 1999; Vollestad et al., 2004). Similar effects occur in other non-salmonid species (Day and Rowe, 2002). To avoid confusion, we note that the mechanisms studied here are neither (1) the indirect effect on survival of varying development rate due to consequent variation in time spent at higher mortality (*e.g.*, Moloney et al., 1994), nor (2) the interaction between age structure and over-compensatory density-dependent recruitment that causes cycles of period roughly twice the generation time (Ricker, 1954; Botsford, 1997).

In the models used here the cyclic mode with period $2T$ does not arise, primarily because of the form of stock-recruitment we use, but the mode with period T turns out to play a central role in our investigation. Recently Myers et al. (1998) explored stochastic forcing of a cyclic mode of variability of period T as a potential cause of observed cycles in sockeye salmon (*Oncorhynchus nerka*) in British Columbia, Canada. This mode is the “echo effect” associated with linear age structured models of semelparous species (Sykes, 1969). They noted that while this mode would not be the dominant mode, it could appear clearly in solutions obtained through forcing by randomly varying survival.

The time scales (or frequency content) of the population response will also depend on the mode of observation, *e.g.*, whether it is a time series of recruitment, abundance or catch (Botsford, 1986; Anderson et al., 2008). The nature of a catch time series will depend on fishing mortality rate, with higher fishing rates leading to higher frequencies of variability (Botsford, 1986; Hsieh et al., 2006). Differences between the spectra of recruitment and abundance of cod have been illustrated by Bjørnstad et al. (2004).

There are several examples of recent attempts to improve understanding of the interactions between nonlinear age-structured models and environmental variability. Generally, these involve forming a linear model by approximating the true model about a fixed point and the mean of the environmental forcing. For example, Greenman and Benton (2003) clarified the issue of “noise amplification,” *i.e.*, excitement of a barely stable mode of variability by an external

driver, by showing how it depended on the spectrum of the noise input and the life history stage at which the environmental noise acted. Bjørnstad et al. (2004) showed how the phenomenon of “cohort resonance,” cyclic behavior due to echoing at a period of one generation time, could lead to an increase in population variance at lower frequencies. This is an issue of importance here because of our interest in potentially slow changes in survival and development due to climate change.

2. Model Formulation

To investigate these questions, we introduce a density-dependent, stochastic age-structured model which we can use to compare the effects of timing of reproduction and annual survivorship of salmon. Let n be the maximum spawning age in years, and let $\vec{x}(t) = (x_1(t), \dots, x_n(t))^T$ be the age-structured population vector at year t . Then our model is

$$\vec{x}(t) = F(\vec{x}(t-1), t) = \begin{pmatrix} R(P(t)) \\ s(t) x_1(t-1) \\ s(t) x_2(t-1) \\ \vdots \\ s(t) x_{n-3}(t-1) \\ (1 - \delta_e(t)) s(t) x_{n-2}(t-1) \\ \delta_l(t) s(t) x_{n-1}(t-1) \end{pmatrix} \quad (1)$$

where $P(t) = (\delta_e(t) x_{n-2}(t-1) + (1 - \delta_l(t)) x_{n-1}(t-1) + x_n(t-1))$ is the number of fish returning to spawn in year t , and

$$R(P(t)) = \frac{\alpha P(t)}{1 + \beta P(t)} \quad (2)$$

is a Beverton-Holt density dependent recruitment term (Beverton and Holt, 1957). Thus $R(P(t))$ represents the number of outmigrants (smolts) leaving a spawning stream in year t , resulting from egg production by individuals of various spawning ages. We have assumed that migration from freshwater to the marine environment occurs in the first year, and that there is no difference in

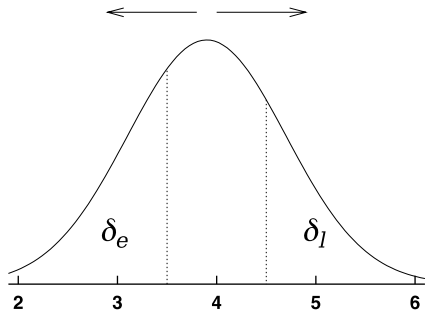


Figure 1: An example illustrating the model representation of the fraction of potential spawners at each age. Here we assume a normal distribution of fraction of potential spawners with mean $a(t) = 3.9$ and $\sigma = 0.8$. The parameters δ_e and δ_l are the integrals over $(-\infty, 3.5]$ and $[4.5, \infty)$, respectively.

fecundity between the different ages of spawning. Parameters α and β characterize the density-dependent reproduction phase: α is the density-independent per-capita growth rate when the population is very small, and $\frac{\alpha}{\beta}$ is the maximum total number of offspring. Timing of reproduction is controlled by the remaining two parameters: most individuals spawn at age $n - 1$; a proportion $\delta_e(t)$ of those that are age $n - 2$ spawn early in year t ; and a proportion $\delta_l(t)$ of age $n - 1$ fish in year t postpone spawning until one year later, when they are age n . Annual survival $s(t)$, as written here, affects all age classes in year t . However, we also explore the possibility that the dominant variability in ocean survival occurs during the period immediately following ocean entry. In that case, the environment affects individual cohorts separately (independently) (Botsford et al., 2005). We account for this possibility in our analysis and compare consequences. Salmon spawning ages are determined by the state of development prior to the age of potential spawning. This is represented by a distribution of spawning ages with a time varying mean $a(t)$ as shown in Figure 1.

3. Model Analysis

In the salmon model (1), we are interested in comparing the effects of fluctuations in annual survivorship and timing of spawning. We do this by studying the case of fluctuating $s(t)$ and the case in which $\delta_e(t)$ and $\delta_l(t)$ depend on the

fluctuating mean age of spawning $a(t)$. In all cases, we consider a time-varying and stationary input signal, $\xi(t)$, and we wish to understand the time scales of variation in the solutions to model (1).

3.1. Linear System

We begin by linearizing about a fixed point $\tilde{\vec{x}}$, and defining $\vec{y} = \vec{x} - \tilde{\vec{x}}$, so that the dynamics of \vec{y} are approximated by

$$\vec{y}(t) \approx \mathbf{J}\vec{y}(t-1) + \sum_{l=0}^L \mathbf{H}(l)\xi(t-l), \quad (3)$$

where \mathbf{J} is the Jacobian matrix of F evaluated at $\tilde{\vec{x}}$ and $\mathbf{H}(l)$ is a constant vector describing the linear effects of the stochastic variable ξ at time lag l on the dynamics of system (1), and $L \leq n$ is the maximum lag of stochastic effects (see the Appendix for a more complete treatment of the mathematical details, including the more general case of a vector-valued forcing signal).

To obtain the conditions for the fixed point, we consider the mean system defined by (1) with $s(t)$, $\delta_e(t)$, and $\delta_l(t)$ all held constant at their average values s, δ_e, δ_l . This system has a unique positive fixed point that is globally attracting for positive trajectories:

$$\tilde{\vec{x}} = \begin{pmatrix} 1 \\ s \\ s^2 \\ \vdots \\ s^{n-3} \\ (1 - \delta_e)s^{n-2} \\ (1 - \delta_e)\delta_l s^{n-1} \end{pmatrix} \frac{\alpha - c}{\beta}, \quad (4)$$

where $1/c = \delta_e s^{n-3} + (1 - \delta_e)(1 - \delta_l)s^{n-2} + (1 - \delta_e)\delta_l s^{n-1}$ is the amount of spawning in the lifetime of the average smolt.

At this fixed point, the Jacobian is

$$\mathbf{J} = \begin{pmatrix} 0 & \cdots & 0 & \delta_e \frac{c^2}{\alpha} & (1 - \delta_l) \frac{c^2}{\alpha} & \frac{c^2}{\alpha} \\ s & & & & & 0 \\ & \ddots & & & & \vdots \\ & & s & & & \vdots \\ & & & (1 - \delta_e)s & & \vdots \\ & & & & \delta_l s & 0 \end{pmatrix}, \quad (5)$$

where all entries left blank are zero.

To model fluctuating survival, we have $s(t) = s + \xi(t)$, with $\xi(t) \in \mathbb{R}$ and $E(\xi(t)) = 0$. In this case, the forcing is captured by the single vector $\mathbf{H}_s(0)$, with

$$\mathbf{H}_s(0) = \left(\frac{\partial F_i}{\partial \xi(t)} \right) = \begin{pmatrix} 0 \\ \tilde{x}_1 \\ \tilde{x}_2 \\ \tilde{x}_3 \\ \vdots \\ \tilde{x}_{n-3} \\ (1 - \delta_e)\tilde{x}_{n-2} \\ \delta_l \tilde{x}_{n-1} \end{pmatrix} = \begin{pmatrix} 0 \\ 1 \\ s \\ s^2 \\ \vdots \\ s^{n-4} \\ (1 - \delta_e)s^{n-3} \\ (1 - \delta_e)\delta_l s^{n-2} \end{pmatrix} \frac{\alpha - c}{\beta}, \quad (6)$$

where s is the mean survival rate, that is, when $\xi(t) = 0$. We note that when survival is forced additively, as we have done here, the deterministic system described above is not exactly the mean of the stochastic system. A stochastic system with $s(t) = se^{\xi(t)}$ would have the deterministic system as its mean, but in the limit of small noise, these representations have identically-shaped frequency responses that merely differ by a factor of s . We chose additive noise for convenience.

For forcing of survival at ocean entry, survival to age 2 will be stochastically

forced, but no other terms are affected, so that

$$\mathbf{H}_{s_e}(0) = \begin{pmatrix} 0 \\ \frac{\alpha-c}{\beta} \\ 0 \\ \vdots \\ 0 \end{pmatrix}. \quad (7)$$

To study fluctuating age of spawning we suppose that individuals' ages of spawning are chosen from a normal distribution that centers on the mean age of spawning $a(t)$ in year t (Fig. 1), specifically

$$p(a - a(t)) = \frac{1}{\sqrt{2\pi}\sigma} e^{-\left(\frac{a-a(t)}{\sqrt{2}\sigma}\right)^2}. \quad (8)$$

We approximate by having all early spawners spawn one year early and all late spawners spawn one year late, so that

$$\delta_e(t) = \int_{-\infty}^{n-1.5} p(a - a(t)) da \quad (9)$$

and

$$\delta_l(t) = \int_{n-0.5}^{\infty} p(a - a(t-1)) da. \quad (10)$$

Note that $\delta_e(t)$ is a function of the mean spawning age in year t , whereas $\delta_l(t)$ is a function of the mean spawning age in year $t-1$. Writing the fluctuating mean age of spawning as $a(t) = a_c + \xi(t)$, we have lag 0 effects from early spawning

$$\mathbf{H}_a(0) = \left(\frac{\partial F_i}{\partial \xi(t)} \right) = \left(\frac{\partial F_i}{\partial \delta_e} \frac{\partial \delta_e}{\partial \xi(t)} \right) \quad (11)$$

and lag 1 effects from late spawning

$$\mathbf{H}_a(1) = \left(\frac{\partial F_i}{\partial \xi(t-1)} \right) = \left(\frac{\partial F}{\partial \delta_l} \frac{\partial \delta_l}{\partial \xi(t-1)} \right). \quad (12)$$

Since $\frac{\partial a(t)}{\partial \xi(t)} = 1$ we have

$$\frac{\partial \delta_e(t)}{\partial \xi(t)} = \int_{-\infty}^{n-1.5} -p'(a - a(t)) da = -p(n - 1.5 - a(t)) \quad (13)$$

and

$$\frac{\partial \delta_l(t)}{\partial \xi(t-1)} = \int_{n-0.5}^{\infty} -p'(a - a(t-1)) da = p(n - 0.5 - a(t-1)). \quad (14)$$

The vector derivatives we need are

$$\left(\frac{\partial F_i}{\partial \delta_e}\right) = \begin{pmatrix} s^{n-3} \frac{e^2}{\alpha} \\ 0 \\ \vdots \\ 0 \\ -s^{n-2} \\ 0 \end{pmatrix} \frac{\alpha - c}{\beta} \quad (15)$$

and

$$\left(\frac{\partial F_i}{\partial \delta_l}\right) = \begin{pmatrix} -(1 - \delta_e) s^{n-2} \frac{e^2}{\alpha} \\ 0 \\ \vdots \\ 0 \\ (1 - \delta_e) s^{n-1} \end{pmatrix} \frac{\alpha - c}{\beta}, \quad (16)$$

where δ_e in the latter expression refers to the “mean” value of δ_e , that is, the value when $\xi(t) = 0$. Substituting (13) and (15) into (11) yields the forcing at lag 0,

$$\mathbf{H}_a(0) = \begin{pmatrix} -p(n - 1.5 - a_c) s^{n-3} \frac{e^2}{\alpha} \\ 0 \\ \vdots \\ 0 \\ p(n - 1.5 - a_c) s^{n-2} \\ 0 \end{pmatrix} \frac{\alpha - c}{\beta}. \quad (17)$$

Substituting (14) and (16) into (12) yields the forcing at lag 1,

$$\mathbf{H}_a(1) = \begin{pmatrix} -p(n - 0.5 - a_c) (1 - \delta_e) s^{n-2} \frac{e^2}{\alpha} \\ 0 \\ \vdots \\ 0 \\ p(n - 0.5 - a_c) (1 - \delta_e) s^{n-1} \end{pmatrix} \frac{\alpha - c}{\beta}. \quad (18)$$

3.2. Change of Coordinates

We now simplify the problem by changing to the natural coordinate system of \mathbf{J} . If \mathbf{U} is the matrix with the right eigenvectors of \mathbf{J} as columns, \mathbf{V} the matrix of left eigenvectors of \mathbf{J} as rows, $\mathbf{UV} = \mathbf{VU} = \mathbf{I}$, and $\mathbf{\Lambda}$ the diagonal matrix of eigenvalues, we can rewrite the linear system (3) as

$$\vec{w}(t) = \mathbf{\Lambda}\vec{w}(t-1) + \sum_{l=0}^L \mathbf{G}(l)\xi(t-l), \quad (19)$$

where $\vec{w} = \mathbf{V}\vec{y}$ and $\mathbf{G}(l) = \mathbf{VH}(l)$. Thus, $\vec{w}(t)$ is the state of the system at time t resolved into the new coordinate system, and the vectors $\mathbf{G}(l)$ represent the stochastic forcing resolved into the new coordinate system. Further details of the change of coordinates can be found in the Appendix.

3.3. Frequency Analysis

Since we are ultimately interested in the response of the model population to a time-varying input signal, we transform the system (19) into the frequency domain, in order to find a transfer function, $T_M(z)$, such that for a scalar measurement $M(t)$ of the population we have

$$\hat{M}(t) = T_M(z)\hat{\xi}(t), \quad (20)$$

where $\hat{M}(t)$ and $\hat{\xi}(t)$ denote the z -transforms of the series of measurements, $M(t)$, and stochastic forcing, $\xi(t)$, respectively. We consider cases in which the scalar measurement is $M(t) = \vec{q}\vec{x}(t)$, where $\vec{q} \in \mathbb{R}^n$ is a row vector giving the contribution of each age class to the measurement. For example, if we are measuring recruitment, then we have $\vec{q} = (1, 0, \dots, 0)$, whereas for total population, we have $\vec{q} = (1, \dots, 1)$. The transfer function, $T_M(z)$, takes on the form

$$T_M(z) = \sum_i \left(m_i \frac{z}{z - \lambda_i} \sum_{l=0}^L g_i(l)z^{-l} \right), \quad (21)$$

where $m_i = \vec{q}\vec{u}_i$ is the scalar product of the measurement vector and the i 'th right eigenvector, and represents the emphasis of each of the independent subsystems (see Appendix) in the measurement $M(t)$ (see Appendix for the derivation of $T_M(z)$).

4. Results

We used this analysis to address questions of general interest regarding the effects of environmental variability, climate change and fisheries on salmon populations. We demonstrate these using parameter values that approximate the two predominant salmon species along the west coast of the contiguous U.S., coho salmon (*Oncorhynchus kisutch*) and chinook salmon (*O. tshawytscha*). We first find the fixed point of system (1), and then identify different modes of variability to be expected based on the various eigenvectors of the Jacobian evaluated at the fixed point. We then present each issue by contrasting a few examples of different frequency responses to reflect how differences in population dynamics and environmental forcing lead to differences in the sensitivity of populations to the time scales of variability in the environment. In most cases these frequency responses display different degrees of the different modes of variability. Following each comparison of frequency responses, we present a comparison of time series of output in response to a time series of white noise as input. These demonstrate the palpable differences that can stem from the more abstract differences in frequency response. The magnitudes of the introduced variability approximate typical observed levels of variability in survival and spawning age structure. The various important issues addressed include differences in response due to: (a) differences in the life history mechanism of the variability (*e.g.*, survival at different ages, spawning age distribution), (b) differences in the type of measurement or observation, and (c) differences due to preconditioning by adult mortality due to fishing or a long term decline in survival due to climate change

Here we have used parameter values that approximate known or likely values for coho and chinook salmon. Survival rates in the ocean are reasonably well known, and we consider three cases: a “typical” value of $0.85y^{-1}$ (Bradford, 1995), a “small” value of $0.28y^{-1}$, and a “very small” value of $0.2y^{-1}$, estimated from more recent observations of coho salmon. Since the “very small” value is not sustainable in the chinook model, that case is not considered. The

distributions of values of α and β have been estimated for coho salmon, but not for chinook salmon (Barrowman et al., 2003), and we use the modes from those distributions ($\alpha = 60$ and $\beta = 0.00017$). In chinook salmon populations in the California Current, individuals typically spawn primarily at a single dominant age, with less spawning at adjacent ages. The dominant age of spawning increases with latitude (Hill et al., 2003). Here we chose dominant spawning at age 4, i.e., $n = 5$ and $a = 4$. Precocious spawning in chinook salmon ranges from 0–10 percent in males and from 0–3 percent in females (Healey, 1991). We use $\sigma = 0.4$, which makes $\delta_e = \delta_l \approx 0.1$. Coho salmon in the California Current spawn predominantly at age 3 with substantial precocious spawning at age 2 and minimal spawning at age 4. Precocious spawning in coho salmon consists almost completely of males, is more variable than in chinook salmon, and can be as high as 30 percent in natural wild populations (Sandercock, 1991). It is not possible to observe the effects of precocious spawning by males on reproduction directly, but for coho salmon, a modification of genetic methods for estimating effective population size indicated the effective proportion of 2-year-olds to be 35 percent in two naturally spawning populations (Doornik et al., 2002). For coho salmon we chose $n = 4$, $a = 2.75$ and $\sigma = 0.2$, which makes $\delta_e \approx 0.1$ and $\delta_l \approx 0.0001$. For stochastic forcing, we use $\sigma_{E_s} = 0.085$ for variability in survival, and $\sigma_{E_g} = 0.2$ for variation in mean spawning age.

4.1. Dynamics near the fixed point

This model with random variables set to their mean values has a unique positive fixed point (4). The condition for a fixed point can be illustrated in terms of the stock-recruitment function and a straight line through the origin with slope equal to the inverse of mean lifetime egg production (Fig. 2). The fixed point lies at the interception of these, allowing clear interpretation of the effects of long-term changes in survival. As mean ocean survival declines, equilibrium egg production declines, and eventually recruitment declines. For the very low survival rate for chinook salmon, the fixed point is zero indicating survival is not adequate for persistence. Because the parameters for the stock-

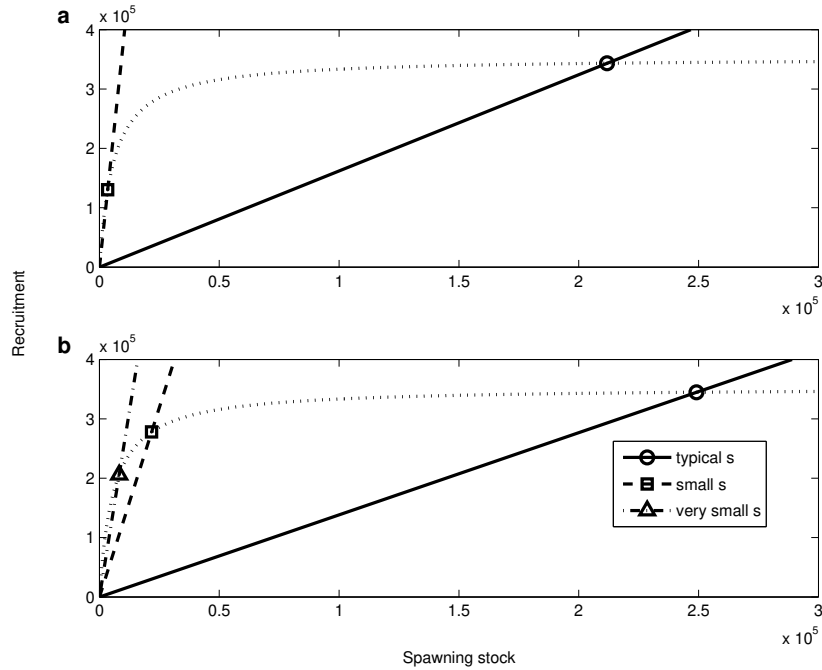


Figure 2: Graphical interpretation of the equilibrium recruitment as the intersection of the smolt-adult curve and a line through the origin with slope $1/(\text{lifetime reproduction})$ for (a) chinook and (b) coho salmon.

recruitment relationship and the estimated survivals are for coho salmon, this has no implications for real chinook salmon populations.

Linearization about a fixed point allows us to describe the dynamics near that point. Figure 3 plots the eigenvalues of the linearization at the fixed point of each of these models. In both the chinook and coho salmon models, the linearized population dynamics responds most strongly to forcing in the one-dimensional mode corresponding to the positive real eigenvalue, λ_1 (the dominant mode of variability). Motion in this mode occurs without oscillation or at low frequencies, and in the direction of the first eigenvector, u_1 , whose entries are all positive. The next strongest mode is a resonance at period $n - 1$ or a little less in the secondary mode (determined by the eigenvalues λ_2 and λ_3 , whose angle from the positive axis is approximately $\pm \frac{2\pi}{n-1}$), indicating oscillations with a

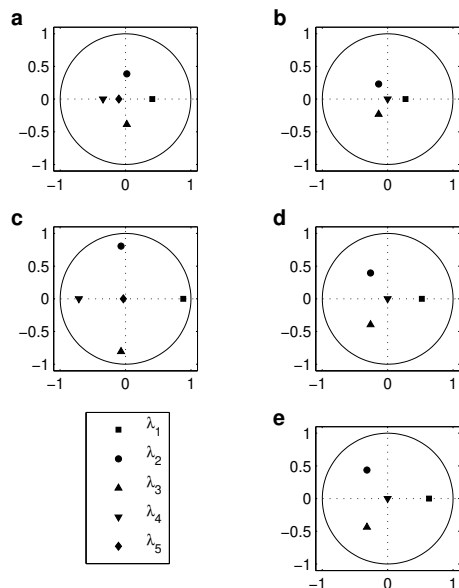


Figure 3: Eigenvalues of linearization matrix \mathbf{J} in chinook and coho models. (a) Chinook, $s = 0.85$, (b) coho, $s = 0.85$, (c) chinook, $s = 0.28$, (d) coho, $s = 0.28$, and (e) coho, $s = 0.2$.

period equal to one generation time. In the chinook case there is also a strong resonance at period two, corresponding to a negative eigenvalue, and in all cases there is a weakly resonating negative eigenvalue as well.

In both the chinook and the coho cases, the effect of decreasing the mean survival is to move all eigenvalues outward toward the unit circle, increasing the return time of all subsystems of interest and thereby increasing the expected magnitude of the cumulative response to variation over time. This effect is especially strong in the chinook model for “small” s (Fig. 3). This occurs because the rate of change of recruitment with adult stock increases as the survival declines (Fig. 2). Thus a small change in spawning stock abundance will result in a larger change in recruitment at low survival than at high survival. Note that rank order of the magnitudes of the dominant eigenvalues are the same as the order of the equilibria, with chinook small survival being the largest, followed by coho very small survival, coho small survival, chinook typical survival then coho typical survival.

The spread in ages of spawning has a relatively small specific influence on the locations of the eigenvalues. When $\sigma = 0$, all fish spawn at age $n - 1$, and the eigenvalues are roots of a simple characteristic polynomial, $P(\lambda) = \lambda(\lambda^{n-1} - s^{n-2}\frac{c^2}{\alpha})$. There is one zero root and the others are equal in size and evenly spaced around zero (not shown). As σ increases, the zero eigenvalue moves outward on the negative real axis, the others move inward slightly and the complex eigenvalues rotate slightly, their polar angles becoming slightly smaller in the chinook case and slightly larger in the coho case (compare chinook and coho salmon in Fig. 3, where σ is larger for chinook salmon). In all cases other than $\sigma = 0$, the positive eigenvalue is largest in magnitude (consistent with the Perron-Frobenius theorem, since the entries of \mathbf{J} are nonnegative).

The responses of this linearized model indicate three important characteristics that determine the responses of salmon populations to environmental variability: (1) the mechanism of environmental forcing, (2) the population variable observed, and (3) long term changes in survival.

4.2. Mechanism of environmental forcing

To demonstrate the difference between population responses to different mechanisms of environmental forcing we compared the cases with: (1) variability in survival in each ocean year, (2) variability in survival at the age of ocean entry and (3) variability in the spawning age distribution. Both frequency responses to environmental variability in survival (Fig. 4) decline from very low frequency, leveling off slightly at a frequency just below that corresponding to period 3 (the dominant age of spawning for coho salmon), then decline for higher frequency. The simulations indicate slightly greater variability than the analytical model in both survival cases. The case with variable ocean survival at all ages is skewed more toward variability at low frequencies. The frequency response to environmental variability in the spawning age distribution increases from low frequency to a resonance at a frequency slightly greater than that corresponding to period three.

The time series for each case (Fig. 5) indicate a clear difference between

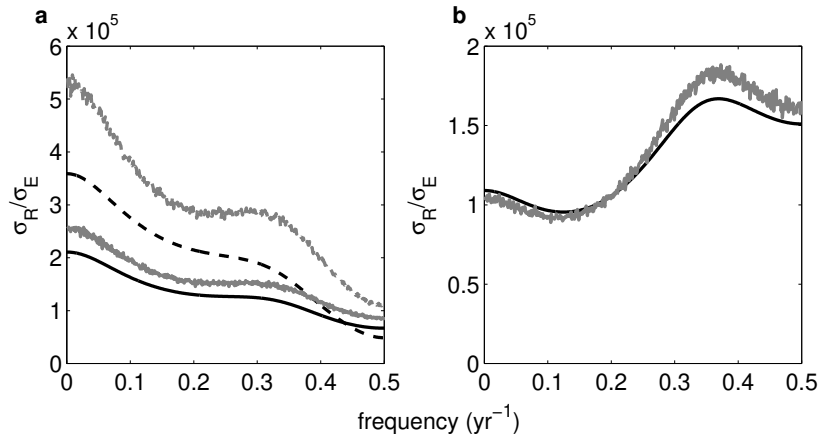


Figure 4: Magnitude of frequency response of recruitment for the linearized model (black lines) and nonlinear simulations (gray lines; 1000 simulations of length 1024) for environmental forcing of (a) early ocean survival rate (solid lines) and ocean survival at all ages (dashed lines), and (b) spawning age distribution for coho salmon with $s = 0.28$.

populations driven by environmental variability in survival and environmental variability in spawning age distribution. The population with environmental forcing of spawning age has clear indications of resonant behavior near period 2 y to 4 y, while the populations with environmental forcing of survival have periods of 5-10 y with little variability. The difference in magnitude between the series with varying survival is as expected from the greater area under the curve in Fig. 4a.

4.3. Population observation

The responses one sees of salmon populations to their environment depend on the type of observation one examines. The most commonly available measurement of salmon populations is annual catch, either in numbers or biomass, and occasionally the age distribution of catch is determined. Frequently catch can be assumed to be individuals who are spawning that year because they are near the mouth of (or in) the spawning river. In some streams, spawning escapement is also estimated, and sometimes the age composition of spawners is also estimated. Catch and escapement can be summed to obtain the total abundance of spawners in a year. Total population abundance at time t cannot

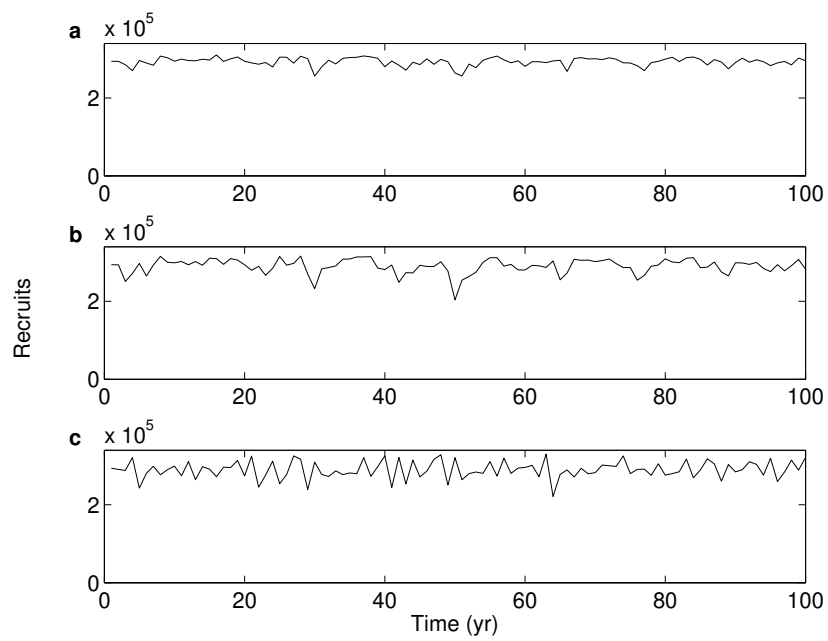


Figure 5: Time series of recruitment in simulations with environmental forcing of (a) early ocean survival ($\sigma = 0.085$), (b) ocean survival at all ages ($\sigma = 0.085$), and (c) spawning age distribution ($\sigma = 0.2$) for coho with $s = 0.28$. Identical sequences of standard normal random variables were used as the forcing signal in order to allow a comparison of filtering by different demographic mechanisms.

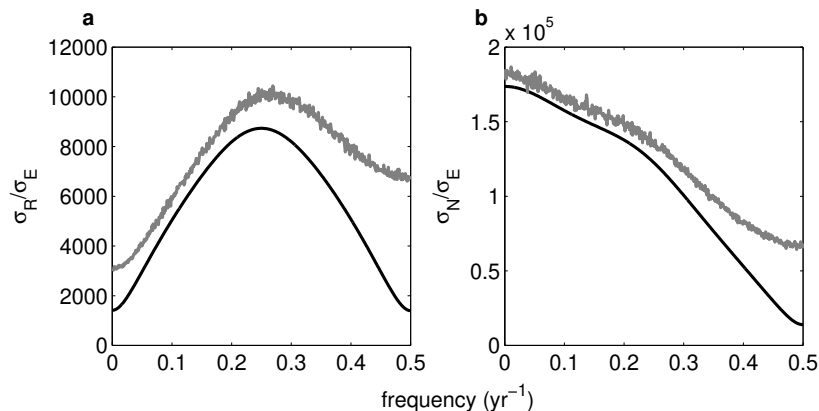


Figure 6: Magnitude of frequency response of (a) recruitment and (b) total abundance for the linearized model (black line) and nonlinear simulations (gray line; 1000 simulations of length 1024) for environmental forcing of spawning age distribution for chinook salmon with $s = 0.85$.

be observed directly, but can be obtained through cohort reconstruction from several years of age-specific data from catch and escapement.

To demonstrate the difference between different types of population observations, we compared the results of observing recruitment with the results of observing total abundance, for chinook salmon with typical survival and environmental variability in the spawning age distribution (Fig. 6). The spectral response of recruitment increases from low frequency to about 0.25yr^{-1} , the period expected for chinook salmon with dominant age of reproduction at 4 y, then declines. The spectral response of total abundance, the sum of several cohorts, declines monotonically from low frequency, showing only a hint of the resonance present in recruitment.

The time series of these two cases (Fig. 7) reflect these characteristics. The time series from the population with observations of recruitment of a chinook salmon population with environmental forcing of spawning age appears to have a preponderance of variability on time scales of 2 y to 5 y, while the time series from the observation of abundance appears to be a smoothed version of that.

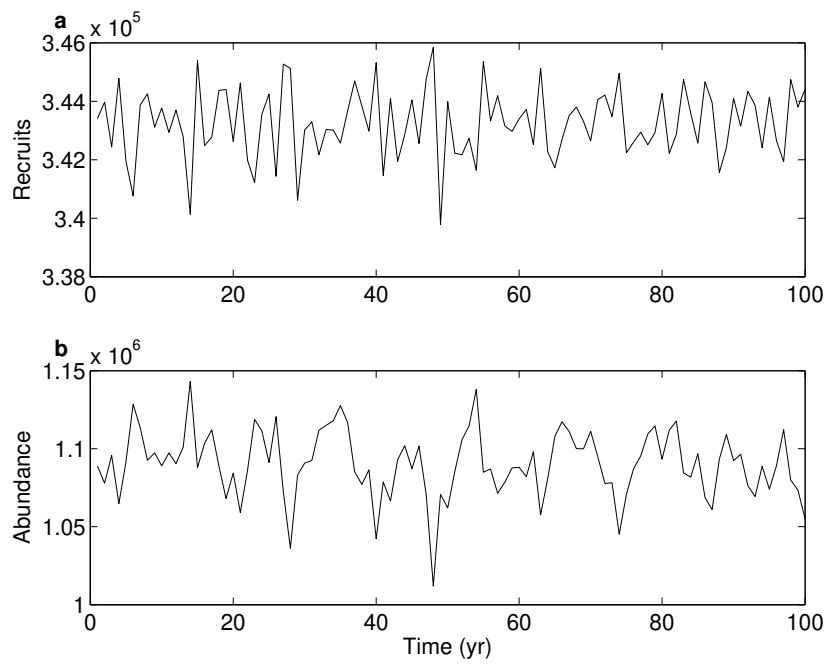


Figure 7: Time series of (a) recruitment and (b) total abundance in a simulation with environmental forcing of spawning age distribution ($\sigma = 0.2$) for chinook salmon with $s = 0.85$.

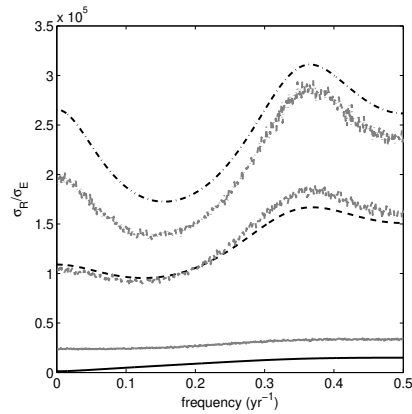


Figure 8: Magnitude of frequency response of recruitment for the linearized model (black lines) and nonlinear simulations (gray lines; 1000 simulations of length 1024 with $\sigma = 0.2$) for environmental forcing of spawning age distribution for coho with $s = 0.85$ (solid lines), 0.28 (dashed lines), and 0.2 (dash-dot lines).

4.4. Long-term mean survival

The effects of long-term changes in survival are of interest for a variety of reasons. The most obvious is concern over the effects of fishing on the response of a population to the environment. Another increasing concern is the effects of changes in environmental variability on decadal time scales. As an example of the latter, ocean survival rates of coho salmon in the California Current declined by an order of magnitude between 1980 and 2000 (Botsford et al., 2005). Both coho and chinook salmon are fished along the west coast of the U.S.

To illustrate the differences between populations operating at different levels of long-term survival we compared the coho salmon recruitment from a model with environmental variability in spawning age distribution with each of the three survival levels, typical, small and very small (Fig. 8). The frequency responses with these three survivals have similar shapes but differ substantially in scale. The resonance at period just less than 3 years is dominant because the variability is in spawning age distribution.

The time series of these three cases (Fig. 9) appear to have similar frequency content, but different levels of variability as expected from Fig. 8. However,

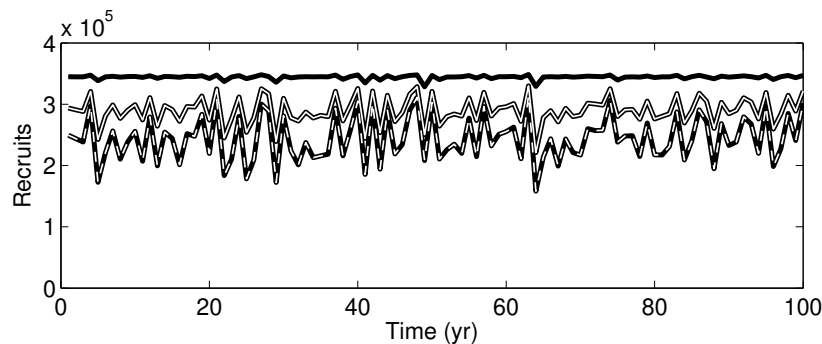


Figure 9: Time series of recruitment in simulations with environmental forcing of spawning age distribution ($\sigma = 0.2$) for coho with $s = 0.85$ (solid black), 0.28 (white with black border), and 0.2 (dashed white on black). Identical sequences of standard normal random variables were used as the forcing signal in order to allow a comparison of filtering at different survival rates.

importantly, they also underscore the fact that as survival declines variability increases as in Fig. 8, as the equilibrium recruitment declines.

5. Discussion

These analyses provide an understanding of how various population characteristics shape the response of salmon populations to variability on various time scales. Salmon population variability does not simply follow variability in the environment as is commonly assumed, but rather the response is shaped by: (a) the life history point of impact of the environment, (b) the specific population observation made, and (c) pre-conditioning by long-term changes in survival. These have important consequences for the management of salmon populations and the anticipation of the effects of large-scale environmental change. The mechanics of salmon responses to the environment are, of course, not unique, but rather are closely related to those of other higher trophic level, age-structured species (McCann et al., 2003; Bjørnstad et al., 2004).

The basic resonance mode with period T (where T is generation time or age of dominant effect on recruitment) is present in deterministic, linear age structured models, as the echo effect (Sykes, 1969; Caswell, 2001), and was

identified earlier as a potential cause of observed cycles in some salmon populations (Myers et al., 1998). Another resonant mode, cycles with period $2T$ was not explored here, but is addressed in many other publications (*e.g.*, Botsford, 1986; McCann et al., 2003; Bjørnstad et al., 2004). That type of cyclic behavior requires a negative slope of the stock-recruitment relationship (overcompensatory), which is not present in the Beverton-Holt form used here (equation (2)). While a Ricker (1954) stock-recruit model is often used because of the ease of fitting, most salmon stock-recruit relationships have a Beverton-Holt form (Beverton and Holt, 1957).

Differences in the dynamic responses of populations to temporal variability at different points in the species life history are not commonly compared. Here the different mechanisms involving variability in survival and variability in spawning age distribution preferentially excited different fundamental modes of variability, and hence these differences were important. In addition to variability in spawning age exciting a completely different mode than variability in survival, differences in responses to varying survival at ocean entry and varying total survival also differed, with lower frequencies resulting from variability in early ocean survival. This can be compared to the difference in population persistence between these two survival mechanisms in earlier analysis (Botsford et al., 2005), where population variability was greater when it occurred at the age of return to the river for spawning, rather than the age of ocean entry of smolts. This occurs because of the Law of Large Numbers, and the fact that the number of spawners is the sum of several random survivals when variability is at the age of entry, but only one random survival when it is at the age of return. Here we would be summing several independent random variables in the case with variability at age of entry and over the same number of variables in the case with random variability at each age, but they would not be independent.

The difference in frequency content between a catch (or abundance) series and a recruitment series was known previously (*e.g.*, Botsford, 1986), but there has been renewed interest in it. That difference basically follows from the Law of Large Numbers and the fact that when recruitment is the source of temporal

variability, abundance will have a lower coefficient of variation because it is the average over several recruitments. As the value of constant harvest rate increases, the number of cohorts averaged over diminishes, and hence higher frequencies are observed. Anderson et al. (2008) recently demonstrated this effect in California fisheries.

An important practical consequence of the results obtained here for the detection of slow changes in climate is that when the models showed increasingly stronger resonance (e.g., as with declining adult survival in Fig. 8), there is also an increase in their sensitivity to very low frequency environmental variability. This means that such populations, even when driven by white noise in the environment, could generate very slowly changing signals that would be difficult to discern from a slowly changing climate. Bjørnstad et al. (2004) drew attention to this after observing it in their model with over-compensatory density dependence at two locations in the life history of Atlantic cod.

The results obtained here provide the means both to begin to explain current differences in responses to the environment by the same species at different locations, and to project differences in future responses on the basis of projected changes in time scales of variability in the environment. Current differences in responses by populations of the same species are typically presumed to imply a difference in environmental forcing, but they may be due to differences in life histories or differences in preconditioning because they are fished at different intensities. Future changes in time scales of variability are expected on the basis of paleological records (e.g., past changes in the time scales of variability of El Niño events as observed in corals and other media Jones et al., 2009) or predictions from global climate models (Timmermann et al., 1999).

Acknowledgments

This research is part of the GLOBEC Northeast Pacific program and was funded by National Science Foundation grants NSF OCE0003254 and NSF OCE0815293.

- Anderson, C., Hsieh, C., Sandin, S., Hewitt, R., Hollowed, A., Beddington, J., May, R., Sugihara, G., 2008. Why fishing magnifies fluctuations in fish abundance. *Nature* 452 (7189), 835–839.
- Barrowman, N., Myers, R., Hilborn, R., Kehler, D., Field, C., 2003. The variability among populations of coho salmon in the maximum reproductive rates and depensation. *Ecological Applications* 13, 784–793.
- Bernstein, D., 1992. Some open problems in matrix theory, arising in linear systems and control. *Linear Algebra and its Applications* (162–164), 409–432.
- Beverton, R., Holt, S., 1957. On the dynamics of exploited fish populations. *Fishery Investigations, Series II. Marine Fisheries*, Great Britain Ministry of Agriculture, Fisheries and Food 19, 533.
- Bjørnstad, O. N., Nisbet, R. M., Fromentin, J. M., 2004. Trends and cohort resonant effects in age-structured populations. *Journal of Animal Ecology* 73 (6), 1157–1167.
- Botsford, L., 1986. Effects of environmental forcing on age-structured populations: northern California Dungeness crab (*Cancer magister*) as an example. *Canadian Journal of Fisheries and Aquatic Sciences* 43 (11), 2345–2352.
- Botsford, L., 1997. Dynamics of populations with density-dependent recruitment and age structure. In: Tuljapurkar, S., Caswell, H. (Eds.), *Structured Population Models in Marine, Terrestrial, and Freshwater Systems*. Chapman and Hall, New York, Ch. 12.
- Botsford, L., Lawrence, C., Hill, M., 2005. Differences in dynamic response of californian current salmon species to changes in ocean conditions. *Deep-Sea Research II* (52), 331–345.
- Botsford, L., Lawrence, C. A., 2002. Patterns of co-variability among californian current chinook salmon, coho salmon, dungeness crab, and physical oceanographic conditions. *Progress in Oceanography* 53, 283–305.

- Bradford, M., 1995. Comparative review of Pacific salmon survival rates. *Canadian Journal of Fisheries and Aquatic Sciences* 52, 1327–1338.
- Caswell, H., 2001. *Matrix population models: construction, analysis, and interpretation*. Sinauer, Sunderland, MA.
- Coronado, C., Hilborn, R., 1998. Spatial and temporal factors affecting survival in coho salmon (*Oncorhynchus kisutch*) in the Pacific Northwest. *Canadian Journal of Fisheries and Aquatic Sciences* 55 (9), 2067–2077.
- Day, T., Rowe, L., 2002. Developmental thresholds and the evolution of reaction norms for age and size at life history transitions. *American Naturalist* 159, 338–350.
- Doornik, D. M., Ford, M. J., Teel, D. J., 2002. Patterns of temporal genetic variation in coho salmon: estimates of the effective proportion of 2-year-olds in natural and hatchery populations. *Transactions of the American Fisheries Society* 131, 1007–1019.
- Elaydi, S. N., 1999. *An Introduction to Difference Equations*, 2nd Edition. Undergraduate Texts in Mathematics. Springer, New York.
- Greenman, J. V., Benton, T. G., 2003. The amplification of environmental noise in population models: causes and consequences. *The American Naturalist* 161 (2), 225–239.
- Healey, M., 1991. Life history of Chinook salmon (*Oncorhynchus tshawytscha*). In: Groot, C., Margolis, L. (Eds.), *Pacific Salmon Life Histories*. UBC Press, Vancouver, Canada, pp. 313–393, 564 pp.
- Hill, M., Botsford, L., Hastings, A., 2003. The effects of spawning age distribution on salmon persistence in fluctuating environments. *Journal of Animal Ecology* 72, 732–744.
- Hsieh, C., Reiss, C., Hunter, J., Beddington, J., May, R., Sugihara, G., 2006. Fishing elevates variability in the abundance of exploited species. *Nature* 443 (7113), 859–862.

- Jones, P., Briffa, K., Osborn, T., Lough, J., van Ommen, T., Vinther, B., Luterbacher, J., Wahl, E., Zwiers, F., Mann, M., Schmidt, G., Ammann, C., Buckley, B., Cobb, K., Esper, J., Goosse, H., Graham, N., Jansen, E., Kiefer, T., Kull, C., Kuttel, M., Mosley-Thompson, E., Overpeck, J., Riedwyl, N., Schulz, M., Tudhope, A., Villalba, R., Wanner, H., Wolff, E., Xoplaki, E., 2009. High-resolution palaeoclimatology of the last millennium: a review of current status and future prospects. *The Holocene* 19 (1), 3–49.
- Logerwell, E., Mantua, N., Lawson, P., Francis, R., Agostini, V., 2003. Tracking environmental processes in the coastal zone for understanding and predicting Oregon coho (*Oncorhynchus kisutch*) marine survival. *Fisheries Oceanography* 12 (6), 554–568.
- McCann, K., Botsford, L., Hastings, A., 2003. Differential response of marine populations to climate forcing. *Canadian Journal of Fisheries and Aquatic Sciences* 60 (8), 971–985.
- Moloney, C. L., Botsford, L., Largier, J. L., 1994. Development, survival and timing of metamorphosis of planktonic larvae in a variable environment: the dungeness crab as an example. *Marine Ecology Progress Series* 113, 61–79.
- Myers, R. A., Mertz, G., Bridson, J. M., Bradford, M. J., 1998. Simple dynamics underlie sockeye salmon (*Oncorhynchus nerka*) cycles. *Canadian Journal of Fisheries and Aquatic Sciences* 55, 2355–2364.
- Pyper, B., Peterman, R., Lapointe, M., Walters, C., 1999. Patterns of covariation in length and age at maturity of British Columbia and Alaska sockeye salmon (*Oncorhynchus nerka*) stocks. *Canadian Journal of Fisheries and Aquatic Sciences* 56, 1046–1057.
- Ricker, W., 1954. Stock and Recruitment. Fisheries Research Board of Canada.
- Sandercock, F., 1991. Life history of coho salmon (*Oncorhynchus kisutch*). In: Groot, C., Margolis, L. (Eds.), *Pacific Salmon Life Histories*. UBC Press, Vancouver, Canada, pp. 397–445, 564 pp.

- Sykes, Z. M., 1969. On discrete stable population theory. *Biometrics* 25 (2), 285–293.
- Teo, S., Botsford, L., Hastings, A., 2009. Spatio-temporal covariability in coho salmon (*Oncorhynchus kisutch*) survival, from California to southeast Alaska. *Deep-Sea Research Part II*.
- Timmermann, A., Oberhuber, J., Bacher, A., Esch, M., Latif, M., Roeckner, E., 1999. Increased El Niño frequency in a climate model forced by future greenhouse warming. *Nature* 398, 694–697.
- Vollestad, L., Peterson, J., Quinn, T., 2004. Effects of freshwater and marine growth rates on early maturity in male coho and chinook salmon. *Transactions of the American Fisheries Society* 133, 495–503.
- Young, K., 1999. Environmental correlates of male life history variation coho salmon populations from two Oregon coastal basins. *Transactions of the American Fisheries Society* 128, 1–16.

Appendix A. General Mathematical Results

The linearization of a stochastic map

$$\vec{x}(t) = F(\vec{x}(t-1), \vec{\xi}(t), \vec{\xi}(t-1), \dots, \vec{\xi}(t-L)), \quad \vec{x}(t) \in \mathbb{R}^n, \quad \vec{\xi}(t) \in \mathbb{R}^m, \quad (\text{A.1})$$

where (without loss of generality) $\mathbb{E}(\xi_i(t)) = 0$, is

$$\vec{y}(t) \approx \mathbf{J}\vec{y}(t-1) + \sum_{l=0}^L \mathbf{H}(l)\vec{\xi}(t-l) \quad (\text{A.2})$$

where $\vec{x}(t) = \vec{\tilde{x}} + \vec{y}(t)$, $\vec{\tilde{x}}$ is a fixed point of $F(\vec{x}, \vec{0})$, $\mathbf{J} = \left(\frac{\partial F_i}{\partial x_j} \right) |_{(\vec{\tilde{x}}, \vec{0})}$ is the Jacobian matrix of F at $\vec{x} = \vec{\tilde{x}}$ and $\vec{\xi} = \vec{0}$, $\mathbf{H}(l) = \left(\frac{\partial F_i}{\partial \xi_j(t-l)} \right) |_{(\vec{\tilde{x}}, \vec{0})}$ is an $n \times m$ matrix, and L is the maximum time lag at which stochastic perturbations affect F directly. Let \vec{v}_i and \vec{u}_i be the left and right eigenvectors, respectively, of \mathbf{J} , and λ_i its eigenvalues. It follows that $\vec{v}_i \mathbf{J} = \lambda_i \vec{v}_i$ and $\mathbf{J} \vec{u}_i = \lambda_i \vec{u}_i$. In this paper we will only deal with matrices that have all distinct eigenvalues. The vector of deviations from equilibrium can be written as a sum of eigenvectors, $\vec{y} = \sum_i w_i \vec{u}_i$.

We change to the natural coordinate system of \mathbf{J} : Let

$$\mathbf{U} = (\vec{u}_1, \dots, \vec{u}_n), \quad \mathbf{V} = \begin{pmatrix} \vec{v}_1 \\ \vdots \\ \vec{v}_n \end{pmatrix}, \quad \mathbf{\Lambda} = \begin{pmatrix} \lambda_1 & 0 & \cdots & 0 \\ 0 & & & \\ \vdots & \ddots & & \vdots \\ 0 & & \cdots & 0 \\ 0 & \cdots & 0 & \lambda_n \end{pmatrix}, \quad (\text{A.3})$$

so that $\mathbf{J} = \mathbf{U}\mathbf{\Lambda}\mathbf{V} = \sum_i \lambda_i \vec{u}_i \vec{v}_i$ and $\mathbf{U}\mathbf{V} = \mathbf{V}\mathbf{U} = \mathbf{I}$. Then for $\vec{w} = \mathbf{V}\vec{y}$,

$$\begin{aligned} \vec{w}(t) &= \mathbf{V}\vec{y}(t) = \mathbf{\Lambda}\mathbf{V}\vec{y}(t-1) + \sum_{l=0}^L \mathbf{G}(l)\vec{\xi}(t-l) \\ &= \mathbf{\Lambda}\vec{w}(t-1) + \sum_{l=0}^L \mathbf{G}(l)\vec{\xi}(t-l) \end{aligned} \quad (\text{A.4})$$

with $\mathbf{G}(l) = \mathbf{V}\mathbf{H}(l)$. Since $\mathbf{\Lambda}$ is diagonal, the dynamics of each $w_i(t)$ is uncoupled from the others:

$$w_i(t) = \lambda_i w_i(t-1) + \sum_{l=0}^L \vec{g}_i(l)\vec{\xi}(t-l) \quad (\text{A.5})$$

where $\vec{g}_i(l) = \vec{v}_i \mathbf{H}(l)$ is row i of $\mathbf{G}(l)$.

Frequency Analysis

For the frequency analysis, take $\vec{w}(j) = \vec{0}$ and $\vec{\xi}(j) = \vec{0}$ for all $j < 0$. Then we may write the z -transform (Elaydi, 1999)

$$\begin{aligned}\hat{w}(z) &\equiv \sum_{k=0}^{\infty} \vec{w}(k) z^{-k} \\ &= \sum_{k=0}^{\infty} \left(\mathbf{\Lambda} \vec{w}(k-1) + \sum_{l=0}^L \mathbf{G}(l) \vec{\xi}(k-l) \right) z^{-k} \\ &= \mathbf{\Lambda} \underbrace{\sum_{k=0}^{\infty} \vec{w}(k-1) z^{-k}} + \sum_{l=0}^L \mathbf{G}(l) \underbrace{\sum_{k=0}^{\infty} \vec{\xi}(k-l) z^{-k}}.\end{aligned}\quad (\text{A.6})$$

The bracketed expressions are themselves z -transforms of shifted sequences of \vec{w} and $\vec{\xi}$, so that by the shift property of the z -transform (Elaydi, 1999),

$$\hat{w}(z) = \mathbf{\Lambda} z^{-1} \hat{w}(z) + \sum_{l=0}^L \mathbf{G}(l) z^{-l} \hat{\xi}(z) \quad (\text{A.7})$$

or

$$\hat{w}(z) = (1 - \mathbf{\Lambda} z^{-1})^{-1} \sum_{l=0}^L \mathbf{G}(l) z^{-l} \hat{\xi}(z). \quad (\text{A.8})$$

$(1 - \mathbf{\Lambda} z^{-1})^{-1}$ is a diagonal matrix with entries $\frac{1}{1 - \lambda_i z^{-1}} = \frac{z}{z - \lambda_i}$. Consequently the z -transformed deviation vector,

$$\hat{y}(z) = \mathbf{U} \hat{w}(z) = \sum_{i=1}^n \left(\vec{u}_i \frac{z}{z - \lambda_i} \sum_{l=0}^L \vec{g}_i(l) z^{-l} \hat{\xi}(z) \right), \quad (\text{A.9})$$

is a linear sum of rational functions of z , with peaks tending to be near the eigenvalues of \mathbf{J} .

Measurement

Assume we are observing the population via a scalar measurement, whether annual total population, recruitment or catch, represented as $M(t) = Q(\vec{x}(t))$. Let us assume that $Q(\vec{x})$ is differentiable at the fixed point $\vec{\tilde{x}}$. In the weak noise limit this quantity also can be described by a linear approximation,

$$\begin{aligned}Q(\vec{x}(t)) &= Q(\vec{\tilde{x}}) + \sum_i \frac{\partial Q}{\partial x_i}(\vec{\tilde{x}}) y_i(t) + \text{O}(|y|^2) \\ &= Q(\vec{\tilde{x}}) + \sum_i q_i y_i(t) + \text{O}(|y|^2).\end{aligned}\quad (\text{A.10})$$

The measurement $M(t)$ is approximated by the linear quantity $Q(\tilde{\vec{x}}) + \sum_i q_i y_i(t)$, which differs by only a constant from $\sum_i q_i x_i(t)$, and fluctuation in either quantity has the same characteristics as fluctuation just in $\sum_i q_i y_i(t)$. Introducing a row vector $\vec{q} = (q_1, \dots, q_n)$, we can represent the linearized measurement as a vector product $\vec{q}\vec{y}(t)$.

Changing to the natural coordinates of \mathbf{J} ,

$$\vec{q}\vec{y}(t) = \vec{q} \sum_j w_j(t) \vec{u}_j = \sum_j \vec{q}\vec{u}_j w_j(t) = \sum_j m_j w_j(t), \quad (\text{A.11})$$

where $m_j = \vec{q}\vec{u}_j$.

Similarly, in the frequency analysis of $M(t)$,

$$\begin{aligned} \hat{M}(z) &= \sum_{k=0}^{\infty} M(k) z^{-k} \\ &\approx \sum_k (Q(\tilde{\vec{x}}) + \sum_i m_i w_i(k)) z^{-k} \\ &= \sum_k Q(\tilde{\vec{x}}) z^{-k} + \sum_i m_i \hat{w}(z). \end{aligned} \quad (\text{A.12})$$

It is appropriate to discard the constant part of $M(t)$ since we are concerned with year to year variation:

$$\begin{aligned} \sum_i m_i \hat{w}(z) &= \sum_i \left[m_i \sum_{l=0}^L \vec{g}_i(l) \frac{z}{z - \lambda_i} z^{-l} \hat{\xi}(z) \right] \\ &= T_M(z) \hat{\xi}(z). \end{aligned} \quad (\text{A.13})$$

The frequency response $T_M(z)$ of the measurement $M(t)$ is a weighted sum of the frequency responses for each subsystem, $T_i(z) = \frac{z}{z - \lambda_i}$, each weighted both by the strength of environmental forcing in that subsystem at each lag, $\vec{g}_i(l)$, and by the ‘‘emphasis’’ of the subsystem in the measurement, m_i .

For a scalar measurement quantity like recruitment or total, as in the body of the paper, the weak noise assumption leads to a linearization

$$Q(\vec{x}(t)) \approx Q(\tilde{\vec{x}}) + \sum_i q_i y_i(t) = Q(\tilde{\vec{x}}) + \vec{q}\vec{y}(t) \quad (\text{A.14})$$

using a row vector \vec{q} . The measurements we consider for the salmon model are in fact linear quantities $Q(\vec{x}(t)) = \vec{q}\vec{x}(t)$: for instance, for total population $\vec{q} = (1, \dots, 1)$ and for recruitment $\vec{q} = (1, 0, \dots, 0)$.

Geometry of measurement and forcing

A particular choice of measurement emphasizes some eigenspaces more than others, and these emphases are summarized by the value of $m_i = \vec{q} \vec{u}_i$ for the different column eigenvectors \vec{u}_i . As an extreme case, if $m_i = 0$, variation in subspace i has no effect at all on the measurement; if m_i is small the effect is small.

To look at measurement geometrically, consider first an extreme case: if \vec{q} is one of the left eigenvectors \vec{v}_i then

$$Q(\vec{x}(t)) = Q(\tilde{\vec{x}}) + w_i(t). \quad (\text{A.15})$$

The fluctuations in Q are the fluctuations in $w_i(t)$, which are the fluctuations in the subspace containing \vec{u}_i . If we decompose the row \vec{q} into a sum of projections \vec{v}_i as $\vec{q} = \sum_i m_i \vec{v}_i = \vec{m} \mathbf{V}$, its components m_i reveal the amount of contribution from each subsystem to the fluctuating quantity $Q(\vec{x}(t)) = Q(\tilde{\vec{x}}) + \sum_i m_i w_i(t)$. If some $m_i = 0$, the corresponding subsystem is ignored by that summary quantity. This is a case of control theory's system observability (Bernstein, 1992).

Similarly, some forcing signals act on some subsystems more than others, characterized by the projection of the forcing into each eigenspace, $\vec{g}_i(l) = \vec{v}_i \mathbf{H}(l)$ for each i and l . This is easiest to illustrate when $L = 0$, so there are no time lags in the forcing signal. In this case, if $\vec{g}_i(0) = 0$ for some i , there is no fluctuation in the subspace containing eigenvector \vec{u}_i , that is, no fluctuation in w_i . If the forcing vector \mathbf{H} is an eigenvector \vec{u}_i , all the fluctuation in the system will be confined to the subsystem containing \vec{u}_i and all the components of \vec{w} other than w_i will be constant. In general, the more the columns of \mathbf{H} are aligned with certain eigenvectors \vec{u} , the more the fluctuations caused by the forcing signal will be concentrated in those subsystems. This is closely related to control theory's system controllability (Bernstein, 1992).